2004

An exploration of aqueous oxalic acid production in the coastal marine atmosphere

Crahan, Kathleen K.; Hegg, Dean; Covert, David S.; Jonsson, Haflidi

ELSEVIER

Atmospheric Environment 38 (2004) 3757–3764

ATMOSPHERIC ENVIRONMENT

www.elsevier.com/locate/atmosenv

An exploration of aqueous oxalic acid production in the coastal marine atmosphere

Kathleen K. Crahan[a,*], Dean Hegg[a], David S. Covert[a], Haflidi Jonsson[b]

[a] *Department of Atmospheric Science, University of Washington, Box 351640, Seattle, WA 98195-1640, USA*
[b] *CIRPAS, 3240 Imjin Rd., Hanger #507, Marina, CA 93933, USA*

Received 9 February 2004; accepted 2 April 2004

Abstract

Oxalic acid is the most abundant dicarboxylic acid found in the troposphere, yet there is still no scientific consensus concerning its origins or formation process. Recent studies have suggested mechanisms for its formation in cloud water from gaseous precursors. Comparison of the characteristics of oxalic acid and nss sulfate, a chemical with a known in-cloud formation pathway, provides some support for an aqueous formation mechanism for oxalic acid. Analysis of the filters collected from the CIRPAS Twin Otter aircraft during CARMA I, a field campaign designed to study the marine stratocumulus off the coast of Monterey, CA, by a five stage Micro-Orifice Impactor (MOI) revealed a peak in the concentration distribution at a diameter of 0.26–0.44 μm, similar to the size distribution found for nss sulfate and corresponding to the droplet mode in the aerosol size distribution. An air-equivalent average of $2.03 \pm 0.47\,\mu g\,m^{-3}$ (standard error) of sulfate was observed in the collected marine cloud water, in excess to below-cloud concentrations by $1.16\,\mu g\,m^{-3}$ on average. This suggests in-cloud production similar in concentration to previous field campaigns in coastal marine atmospheres. Oxalate was observed in the clouds at air-equivalent concentrations of $0.21 \pm 0.04\,\mu g\,m^{-3}$, in excess to below-cloud concentrations by $0.14\,\mu g\,m^{-3}$ and suggesting an in-cloud production as well. The tentative identification in cloud water of one of the intermediate species in the aqueous oxalate production mechanism lends further support to an in-cloud oxalate source.

Keywords: Cloud chemistry; Aerosol; Mechanism; California; Dicarboxylic acid

1. Introduction

Oxalic acid, a C2 dicarboxylic acid, is the most abundant dicarboxylic acid in aerosols in both urban and remote atmospheres, and is often a significant contributor to the overall particulate organic mass. Although oxalic acid is known to be a byproduct of automobile exhaust, its omnipresence in remote atmospheres, coupled with its limited estimated lifetime of six to eight days, suggest either a background primary source or a mechanism for its formation from natural precursors. Recently, two pathways for oxalic acid formation in cloud water have been proposed by Warneck (2003) (see Fig. 1). However, little evidence is currently available to support in-cloud oxalate production. In this analysis, we present recent measurements from marine stratocumulus that do provide such support.

2. Study venue and instrumentation

All of the data utilized here were gathered during Cloud-Aerosol Research in the Marine Atmosphere I

*Corresponding author. Tel./fax: +1-206-543-0308.
E-mail address: katie@atmos.washington.edu (K.K. Crahan).

1352-2310/$ - see front matter © 2004 Elsevier Ltd. All rights reserved.
doi:10.1016/j.atmosenv.2004.04.009

(CARMA I), which took place off the California coast in August and September of 2002, as shown in Fig. 2. The Center for Interdisciplinary Remotely Piloted Aircraft Studies (CIRPAS) Twin Otter aircraft was the primary research platform used for data collection and was equipped with a number of instruments to quantify meteorological conditions, cloud properties, gas phase concentrations and aerosol physical and chemical properties. Included in these instruments were the modified Mohen slotted cloud water collector as described by Hegg and Hobbs (1986), a Micro-Orifice Impactor (MOI, MSP, model 4100) and an aerosol filter sampler connected to the Twin Otter air intake probe with an approximate $D_{50\%}$ transmission efficiency of 8 μm diameter. The MOI is a five-stage impactor with $D_{50\%}$ of 2.5, 1.4, 0.77, 0.44 and 0.26 μm and a backup filter. The inlet $D_{50\%}$ is approximately 3.5 μm.

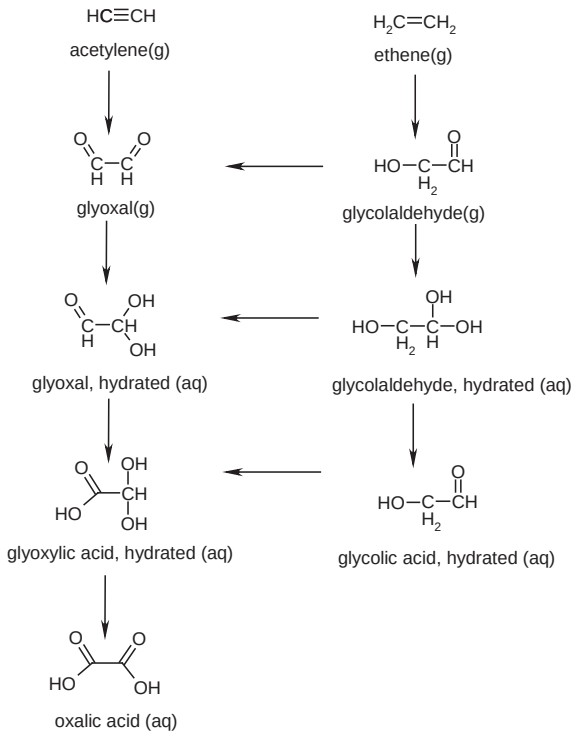

Fig. 1. The proposed reaction pathway for the formation of oxalic acid in-cloud water (Warneck, 2003).

The clouds observed during CARMA I were typically broken over the flight distance of 10–20 km and lasted at least for our sampling period of approximately 20–30 min. The clouds were fairly shallow but moist, typical of tradewind Stratocumulus/Cumulus. A total of 17 cloud water samples and 29 Zeflour 90 mm filter samples were collected, and the MOI, utilizing Zeflour 70 mm filters and a 90 mm backup filter, was employed during three flights. The cloud water samples were treated immediately after collection with a nominal 200 μl of chloroform to prevent further processing of organics by bacteria, and stored at a nominal 5°C in a refrigerator until laboratory analysis. The filters were stored in sterilized petri dishes lined with aluminum foil, and stored in the refrigerator at a nominal 5°C. Filter blanks were collected by using filters that were handled prior, during, and after the field campaign in a manner similar to the filter samples. The blanks had a standard deviation for sulfate and oxalate of 8.0 and 1.3 ppb, respectively. For a collection time of 30 min and a flow

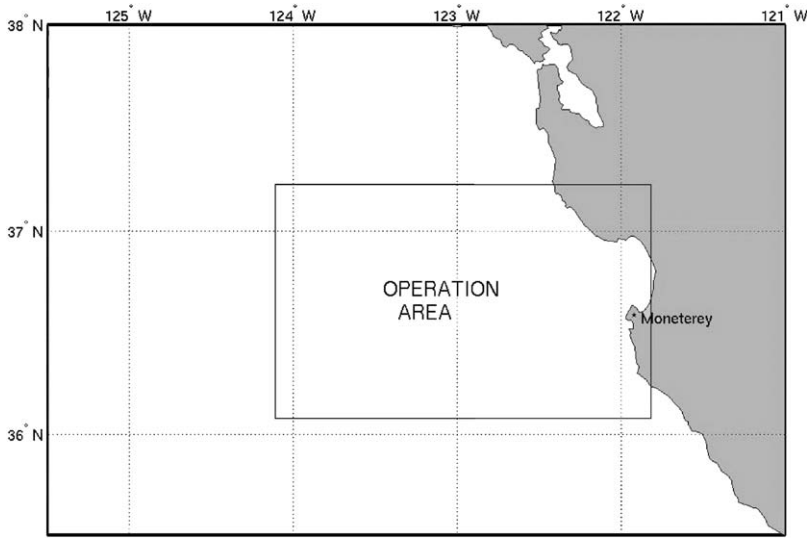

Fig. 2. The area of operation for CARMA I.

rate of 125 lpm, this would translate to a concentration of 0.02 μg SO_4^{2-} m^{-3} and 0.003 μg oxalate m^{-3}. Cloud blanks were collected by passing high-grade HPLC water through the Mohen slotted cloud water collector, and had a standard deviation of 0.59 μg SO_4^{2-} cl^{-1} (10 cl = 1 l) and 0.47 μg oxalate cl^{-1}. The blanks were used to subtract backgrounds accumulated during handling. The chemical speciation of these aerosols was determined in the laboratory as described by Gao et al. (2003), including the use of ion chromatography (IC, model DX-500, Dionex, Sunnyvale, CA) with an eluent of water with a gradient of NaOH increasing from 0.5 to 8 mM over 30 min. Three times the standard deviation of the blanks in solution was used as the detection limit for the aerosols. The errors associated with these two ions were 4% and 6%, respectively. The date, time and altitude of the samples used in this paper are detailed in Table 1.

Additionally, aerosol number-size distributions were determined during the flights with an external Passive Cavity Aerosol Spectrometer Probe 100X (PCASP, PMS/DMT Inc., Boulder, Co) and an external Forward Scattering Spectrometer Probe 100 (FSSP, PMS/DMT Inc., Boulder, CO). The PCASP was used to measure aerosols with diameters between 0.100 and 3.17 μm, the FSSP was configured for course mode aerosol measurements, with lower and upper diameter bounds of 2.00 and 40.4 μm, respectively. A Cloud Imaging Probe (CIP, DMT Inc., Boulder, CO) and a cloud aerosol precipitation spectrometer (CAPS, DMT Inc., Boulder, CO) were also used aboard the Twin Otter. The CAPS measured aerosol concentrations between diameters of 0.5 and 54.9 μm and the CIP was configured specifically to recognize in-cloud drizzle, using lower and upper diameter bounds of 15.4 and 1562 μm, respectively. The FSSP and PCASP were calibrated using glass and latex beads of known diameter and refractive index, as described by Liu et al. (1992). Mass-size distributions were derived from these data assuming an average aerosol density of 1.9 g cm^{-3}.

Table 1
Date, time and altitude each sample was taken and the duration of the exposure time

Date	Sample type	Avg. Altitude (m)	Time start (local)	Duration (min)
24 Aug. 2002	TO	180	13:01	38
	CW #1	520	12:16	3
	CW #2	530	12:29	3
	CW #3	430	12:38	3
26 Aug. 2002	MOI	50	14:15	70
28 Aug. 2002	TO	240	15:09	25
	CW #1	360	12:58	4
	CW #2	410	13:16	4
29 Aug. 2002	TO	180	12:19	46
	CW #1	410	12:19	6
	CW #2	400	12:28	3
30 Aug. 2002	TO	90	13:46	33
	CW #1	290	14:32	6
	CW #2	290	14:40	3
31 Aug. 2002	MOI	50	12:37	67
	TO	180	13:51	38
	CW #1	410	14:46	5
	CW #2	240	15:05	9
3 Sept. 2002	TO	200	10:40	22
	CW #1	290	11:12	4

TO corresponds to a Twin Otter aerosol filter sample, CW corresponds to a cloud water sample, and MOI is a size-resolved Micro-Orifice Impactor sample.

3. Results and discussion

The first piece of evidence supporting the proposed cloud–water formation mechanism is the similarity in the size distribution of the sulfate-containing aerosols and oxalate-containing aerosols in the below-cloud aerosol samples taken by the MOI. Figs. 3 and 4 illustrate that the peaks in mass concentration in both nss sulfate and oxalate size distribution are found between aerosol diameters of 0.26 and 0.44 μm. This is reflected in the smoothed PCASP derived mode with a slightly smaller mean diameter between 0.2 and 0.3 μm. This is likely to be the "cloud droplet residue mode", formed by evaporating cloud droplets (Kerminen and Wexler, 1995; Blando and Turpin, 2000). To assess this further, two methods were employed to estimate the aerosol size distribution resulting from cloud processing in the current data set.

In order to estimate an aerosol droplet mode size distribution, the data from the in-cloud droplet size distribution measured by the FSSP, the chemistry of the droplets determined in the laboratory, and the below-cloud aerosol size distribution measured by the PCASP are available. A typical in-cloud droplet size distribution is seen in Fig. 5. However, as a number of assumptions must be made when doing the calculations, both an upper and lower bound for the aerosol droplet mode size distribution should be estimated. An initial estimate for the aerosol droplet mode size distributions was made by assuming a uniform, internally mixed chemical distribution within the cloud water droplets. The chemical concentrations in the bulk cloud water samples collected with the Mohen sampler were determined through chemical analysis, as detailed by Gao et al. (2003), identifying three monocarboxylic acids, four dicarboxylic acids, four carbohydrates, four inorganic anions, and nine metals. Assuming manganese, zinc, calcium and iron were present in their oxide form, the total chemical mass was determined and divided by a density of 1.9 g cm^{-3} to get residual aerosol volume. The appropriately scaled result, assuming spherical particles,

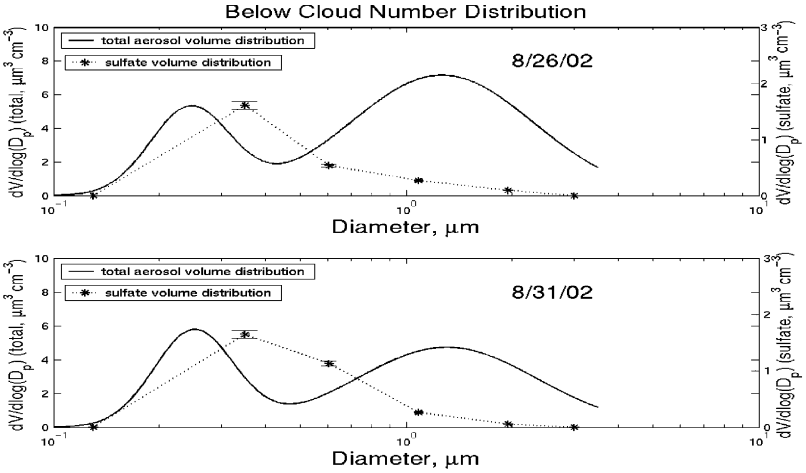

Fig. 3. Comparison of total aerosol mass-size distribution from smoothed PCASP data and simultaneous nss sulfate aerosol mass-size distributions derived from MOI data. Volume was calculated from nss sulfate mass measurements assuming a density of 1.77 g cm^{-3}.

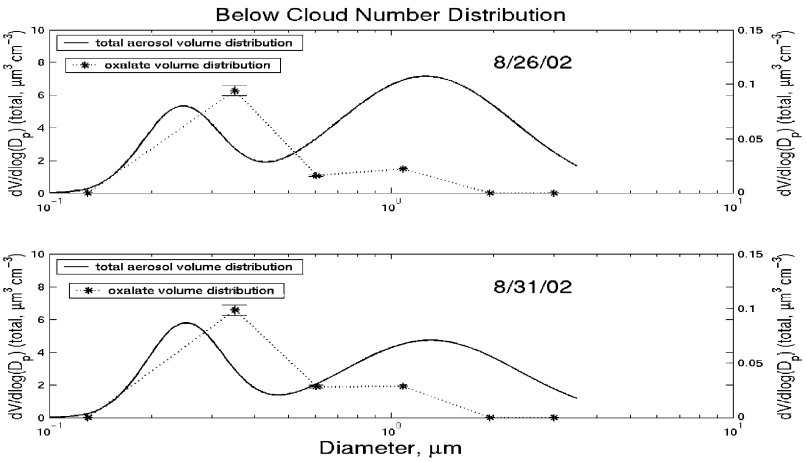

Fig. 4. Comparison of total aerosol size distribution from smoothed PCASP data and simultaneous oxalate aerosol size distributions derived from MOI data. Volume was calculated from oxalate mass measurements assuming a density of 1.9 g cm^{-3}.

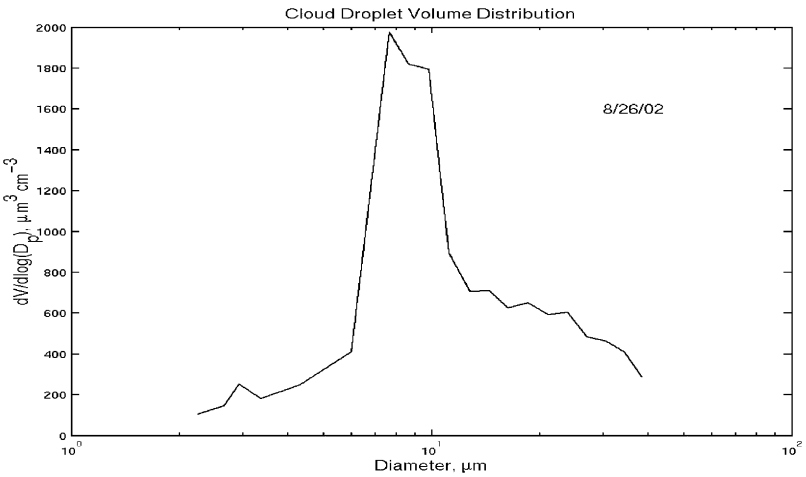

Fig. 5. A typical in-cloud droplet size distribution measured by the FSSP on the 26th of June 2002.

was multiplied by the in-cloud FSSP droplet size distribution, with the end product reflecting the idealized, homogenous aerosol size distribution within the cloud water. The presumed cloud droplet residue particles for the cloud water sampled on the 31st of August had a geometric mass mean diameter of 0.46 μm and a geometric standard deviation of 0.19 μm. However, because the assumption of a uniform chemical distribution within the aerosols is obviously faulty, especially as sea salt is likely dominant in the coarse mode in the marine atmosphere sampled, this should serve as an upper diameter bound for the droplet mode. There was no chemical analysis of the cloud water collected on the 26th of August due to the small sample size.

A lower bound for the aerosol diameter of the droplet mode can be established by comparing the total number concentration of cloud droplets observed by the FSSP in-cloud to the aerosol number observed below-cloud by the PCASP during the MOI collection period. The number distribution observed by the PCASP was summed beginning at the highest channels and adding the lower channels until the PCASP number distribution was equal to or greater than the FSSP in-cloud number distribution. This can be used as an estimate for the lower cut-off diameter for CCN activation. This lower bound was found to fall in PCASP channel four (0.1355–0.1483 μm) on the 26th of August and PCASP channel two (0.1119–0.1220 μm) on the 31st of August. As can be seen in Figs. 3 and 4, the observed sulfate and oxalate volume distribution peaks on these two dates fall well within the upper and lower bounds discussed above. Sufficiently long sample times for significant mass deposition on the MOI substrates occurred on only two of the three MOI samples collected.

The in-cloud and below-cloud total concentrations of nss sulfate and oxalate were compared, and the results are reported in Fig. 6. The cloud droplet sample concentration per unit volume of air was found by multiplying the average cloud liquid water content (LWC) determined by the FSSP with the cloud water chemical concentration as determined from IC analysis. On average, over twice as much sulfate was found in-cloud than below-cloud, which we attribute to in-cloud sulfate production. Subtracting the below-cloud nss sulfate concentration from the in-cloud nss sulfate concentration yielded an average in-cloud sulfate production of $1.16 \pm 0.44\,\mu g\,m^{-3}$ (standard error), which is comparable to the production observed by Hegg and Hobbs (1988) for the Pacific Northwest Coast ($0.97 \pm 0.33\,\mu g\,m^{-3}$). Similarly, there is approximately three times as much oxalate found in-cloud as there is below-cloud and an in-cloud excess of $0.14 \pm 0.03\,\mu g\,m^{-3}$ (standard error), suggesting an in-cloud production pathway for oxalate as well.

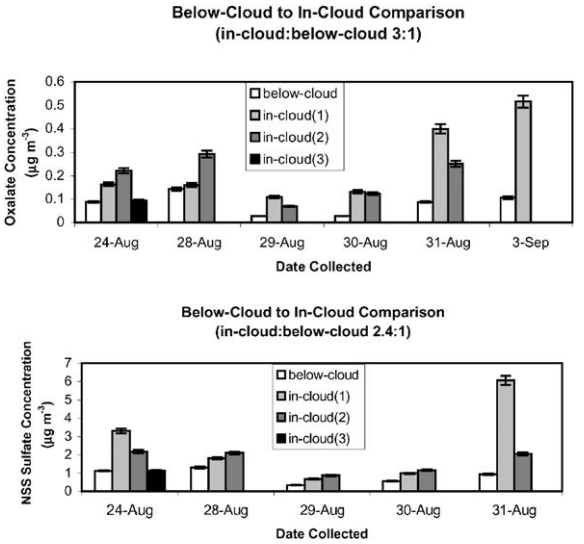

Fig. 6. A comparison of in-cloud to below-cloud concentrations. The upper panel shows the in-cloud excess of the air-equivalent oxalate concentrations as compared to samples collected below-cloud, while the lower panel shows a similar pattern for nss sulfate concentrations. Up to three samples were taken and analyzed for a single cloud. The error bars associated with the concentrations were calculated based upon instrumental uncertainty.

Further support for the aqueous formation pathway of oxalic acid can be obtained by identifying the intermediates for the reaction in the collected cloud water samples through chemical analyses. Although such analyses were not initially carried out, the IC data collected for the cloud water samples were later reviewed to address this question. Due to the time elapsed between the initial analysis of the cloud water and the subsequent search for oxalic acid production precursors, reanalysis of the cloud water using the IC was infeasible because of the breakdown of the organic acids. At the time of reanalysis, a set of standards were run through the IC to ascertain the elution time of glyoxylate and the concentrations at which glyoxylic acid was found in the cloud water samples. The location (retention time) of the glycolate peak was commonly subsumed in the formate peak for the analytical conditions (e.g. eluent strength, flow rate, etc.) at which the cloud water was analyzed. Similarly, the glyoxylic acid peak may also have been engulfed within a strong chloride peak. Nevertheless, when the in-cloud chloride concentration was less than $55\,\mu g\,cl^{-1}$, a peak, attributable to glyoxylate, was detected on the leading shoulder of the chloride peak in five of the 17 cloud water samples. A similar peak was not detected in the aerosol samples collected below cloud, as would be expected due to the limit of detection of the IC for glyoxylic acid if corresponding concentrations of glyoxylic acid were present in the aerosol.

While encouraging, the comparison between field samples and standards run after the sample analysis does raise several issues. First, what additional uncertainty in concentration due to instrumental drift should be applied and, second, how confident of the actual identification of the oxalate intermediary based upon the retention time should we be? Instrumental drift of the IC is caused by subtle variations in the mobile phase and stationary phase column and affects the instrumental response rate and therefore impacts the external calibration used to estimate analyte concentration. In order to account for instrumental drift over time error bars were calculated using a Taylor expansion, with drift estimated from the drift of the slope ($\delta m = 8.5 \times 10^{-5}$) and y-intercept ($\delta b = 6.86$) of the C2–C5 dicarboxylic acid regression analyses from three previous campaigns spanning three years. Reproducibility error was also estimated using one cloud water sample containing the glyoxylate peak from the 23rd of August that was analyzed three times in the IC immediately following the CARMA I field campaign. However, it was the y-intercept drift that dominated the error, with all samples yielding an uncertainty of $\pm 0.07\,\mu g\,cl^{-1}$.

The time between the initial analysis of the cloud water and the subsequent identification of the glyoxylate peak, coupled with the one-dimensionality of the chemical analysis technique leads to only a tentative identification of the glyoxylic peak. Due to IC instrumental drift over time, the peak retention time is simply not an decisive way to identify an analyte. However, the IC selectivity factor can also be used to support the existence of the glyoxylate peak. The selectivity factor is a ratio of k for two different analytes within the same analysis, where k is the ratio of moles of the analyte in the mobile phase of the IC analysis to the moles in the stationary phase. This can be estimated by subtracting the dead time of the IC run from the retention time and then dividing the difference by the dead time, leading to the following equation:

$$\alpha = (t_{r,Cl} - t_{0,Cl})/(t_{r,g} - t_{0,g}), \quad (1)$$

where α is the selectivity factor, t_r the retention time, t_0 the dead time, and the subscripts Cl and g refer to chloride and glyoxylic acid, respectively. This can provide support for the glyoxylic peak identification as it is independent of the volume of the stationary phase and mobile phase. The two standards that contained both glyoxylic acid and chloride had a mean selectivity factor of 1.22 ± 0.01 (standard deviation), while the five cloud water samples had a mean of 1.25 ± 0.03.

The results of the glyoxylic acid IC analysis with corresponding oxalate peaks are seen in Fig. 7. The anomalously high oxalate peak observed on the 23rd of August corresponds with relatively high concentrations of malonic, succinic and glutaric acids. The presence of levoglucosan in the sample, not found in any of the other samples shown in Fig. 7, suggests that an additional source of dicarboxylic acids may be present in this sample due to biomass burning. A haze layer was observed that day above the cloud top and satellite imagery (MODIS 14 Terra, Collection 04) confirm large fires in the area at the time of the campaign.

It is also important to assess how internally consistent the observed glyoxylic acid and oxalic acid levels are with the Warneck mechanism. Warneck (2003) suggested a rate constant of $1.84 \times 10^{-4}\,s^{-1}$ for the in-cloud reaction of hydrated glyoxylic acid to oxalic acid. Assuming steady state and an open system such that the concentration of glyoxylic acid is constant, the amount of oxalic acid expected given a concentration of glyoxylic acid can be calculated using the following equation:

$$[Ox] = k[Gly]ft, \quad (2)$$

where [Ox] is the concentration of oxalic acid, [Gly] the concentration of glyoxylic acid, k the rate constant, f the fraction of time the air parcel spends in the cloud, and t the residence time of the aerosol in the troposphere. For specific cases, f can be estimated as the vertical fraction of the marine boundary layer occupied by the stratocumulus cloud deck determined using the FSSP and CAPS hotwire probe vertical profile measurements of total aerosol volume. A value of 6–8 days was assigned to t based upon similar size distributions of the aerosols containing sulfate and oxalate and the calculations by Hoppel et al. (1990) for atmospheric residence time of aerosols of a given diameter. Using the suggested rate constant and the concentration of glyoxylic acid observed in the cloud water samples collected during CARMA I a concentration of 0.47–1.17 $\mu mol\,cl^{-1}$ oxalic acid is predicted for the samples. However, the measured oxalic acid concentrations are an order of magnitude less, ranging from 0.03–0.13 $\mu mol\,cl^{-1}$, as seen in Fig. 8. Several possibilities exist that could explain this discrepancy in the oxalate concentrations. The simplified equation assumes that the concentration of glyoxylic acid in-cloud water does not change whereas in reality glyoxylic acid may be depleted at a rate faster than it can be replenished. Furthermore, the only sink modeled in Warneck's (2003) calculations is the globally averaged precipitation scavenging term, whereas conditions at Monterey suggest rainout at a much faster rate. Additionally, drizzle would deplete the oxalate to glyoxylate ratio as it naturally favors the larger and therefore older cloud droplets where oxalate production is closest to equilibrium. Comparing the vertical profile of the cloud LWC to the adiabatic LWC profile, calculated from in situ measurements of pressure and temperature and using Teten's equation to estimate vapor saturation, a significant discrepancy that could be attributable to rain-out is noticeable in the profiles collected on the 22nd and 29th of August. This is further

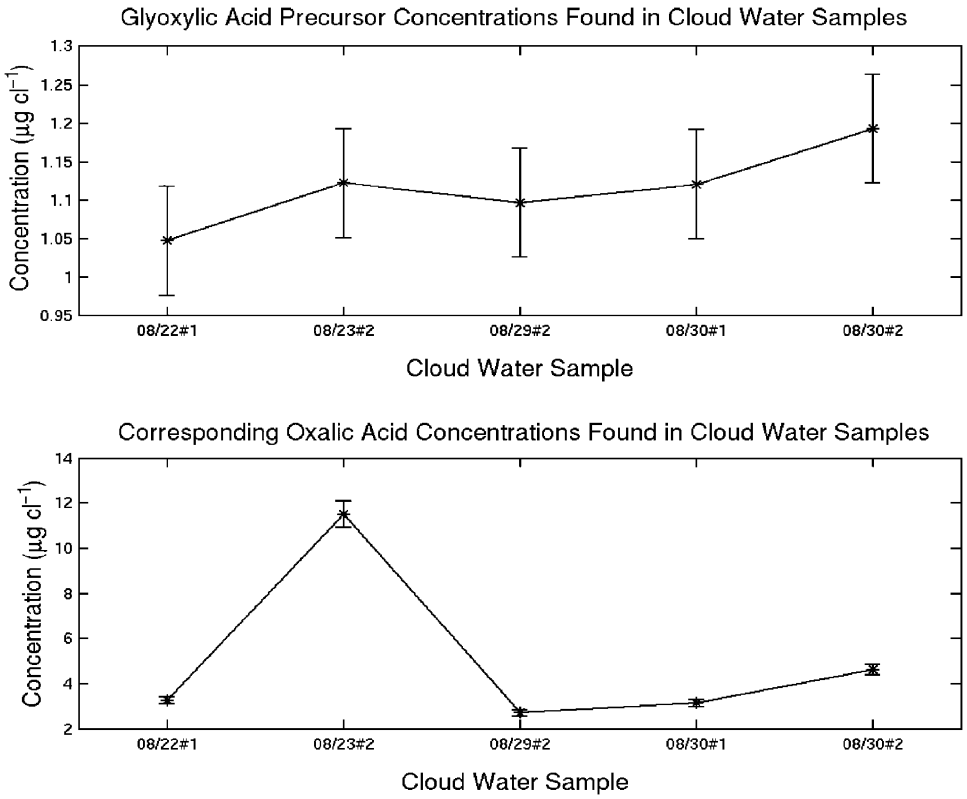

Fig. 7. Glyoxylic acid and oxalic acid concentrations and associated error bars identified in-cloud water samples using ion chromatography detection techniques.

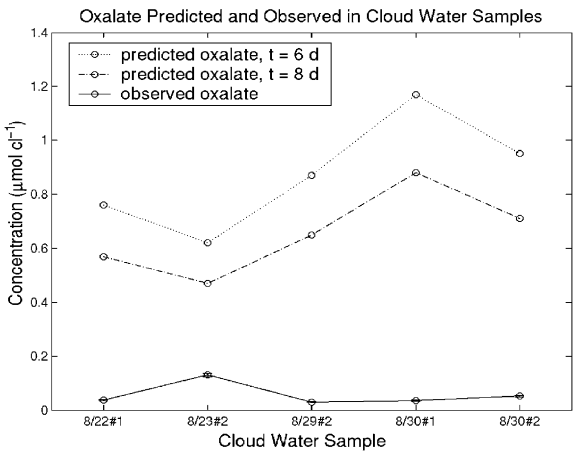

Fig. 8. Calculation of the predicted oxalate using the observed glyoxylate cloud water concentrations and Eq. (2), assuming a residence time (t) of six to eight days based upon the observed size distributions of oxalate and the calculations of Hoppel (1990). The observed vertical fraction of the MBL occupied by the stratocumulus cloud deck used in the calculations varied from 0.40 to 0.75.

confirmed by the CIP vertical profiles of those clouds, which are consistent with in-cloud drizzle. If a closed system were assumed, the maximum amount of oxalic acid produced from the given glyoxylic acid concentration would be scarcely more than the initial glyoxylic acid concentration. The observed oxalic acid concentration falls within these two bounds.

4. Conclusion

The results presented above support the possibility of an aqueous production pathway for oxalic acid, and suggest several possible implications. While the oxalic acid contributes only a small portion to the total mass of the aerosol population (less than 3% on average during CARMA I), it may contribute a significant amount to the smaller sized aerosol population, increasing their diameter and thus the number of cloud condensation nuclei available for activation, possibly impacting cloud albedo and cloud lifetime. Based upon model results, Anttila and Kerminen (2002) claimed that mixing ratios equivalent of oxalic acid larger than 100 pptv would have a significant

positive impact on cloud droplet activation, changing the number of activated cloud droplets approximately 7–30% in the marine atmosphere, dependent upon the updraft velocity. While the below-cloud mixing ratios of oxalic acid were on average only 25 pptv, in-cloud air-equivalent mixing ratios were above 100 pptv in five cases. Furthermore, assuming all of the dicarboxylic acids have a similar effect on CCN activation, six additional cases were above 100 pptv when examining the total C2–C5 dicarboxylic acid mixing ratio. Based upon the data gathered by the CARMA I field campaign, further study of the aqueous production pathway of oxalic acid and its implications is warranted.

Acknowledgements

Support for this research was provided by ONR grant N00014-97-1-0132 and NSF grant ATM 9908471.

References

Anttila, T., Kerminen, V., 2002. Influence of organic compounds on the cloud droplet activation: a model investigation considering the volatility, water solubility, and surface activity of organic matter. Journal of Geophysical Research 107 (Art.), 12.

Blando, J.D., Turpin, B.J., 2000. Secondary organic aerosol formation in cloud and fog droplets: a literature evaluation of plausibility. Atmospheric Environment 34, 1623–1632.

Gao, S., Hegg, D.A., Covert, D.S., Jonsson, H., 2003. Aerosol chemistry, and light-scattering and hygroscopicity budgets during outflow from East Asia. Journal of Atmospheric Chemistry 46, 55–88.

Hegg, D.A., Hobbs, P.V., 1986. Sulfate and nitrate chemistry in marine cumuliform clouds. Atmospheric Environment 20, 901–909.

Hegg, D.A., Hobbs, P.V., 1988. Comparisons of sulfate and nitrate production in clouds on the mid-Atlantic and Pacific Northwest Coasts of the United States. Atmospheric Chemistry 7, 325–333.

Hoppel, W.A., Fitzgerald, J.W., Frick, G.M., Larson, R.E., Mack, E.J., 1990. Aerosol size distributions and optical properties found in the marine boundary layer over the Atlantic Ocean. Journal of Geophysical Research—Atmospheres 95, 3659–3686.

Kerminen, V.M., Wexler, A.S., 1995. Growth laws for atmospheric aerosol particles: an examination of the biomodality of the accumulation mode. Atmospheric Environment 29, 3263–3275.

Liu, P.S.K, Leaitch, W.R., Strapp, J.W., Wasey, M.A., 1992. Response of particle measuring systems airborne ASASP and PCASP to NaCl and latex particles. Aerosol Science and Technology 16, 83–95.

Warneck, P., 2003. In-cloud chemistry opens pathway to the formation of oxalic acid in the marine atmosphere. Atmospheric Environment 37, 2423–2427.